Local Exergy Cost analysis of cullet glass heating by microwaves

Luis Acevedo[a], Sergio Usón[b*], Javier Uche[c]

[a]Research Centre for Energy Resources and Consumption (CIRCE), *Zaragoza, Spain, lacevedo@fcirce.es*
[b]Department of Mechanical Engineering, CIRCE Institute, Universidad de Zaragoza, *Zaragoza, Spain, suson@unizar.es*
[c]Department of Mechanical Engineering, CIRCE Institute, Universidad de Zaragoza, *Zaragoza, Spain, javiuche@unizar.es*

* Corresponding address: Betancourt Building. María de Luna St, 50018 Zaragoza (Spain).
Phone: +34 876 55 5216

Local Exergy Cost analysis of cullet glass heating by microwaves

Luis Acevedo[a], Sergio Usón[b], Javier Uche[c]

[a]Research Centre for Energy Resources and Consumption (CIRCE), *Zaragoza, Spain, lacevedo@fcirce.es*
[b]Department of Mechanical Engineering, CIRCE Institute, Universidad de Zaragoza, *Zaragoza, Spain, suson@unizar.es*
[c]Department of Mechanical Engineering, CIRCE Institute, Universidad de Zaragoza, *Zaragoza, Spain, javiuche@unizar.es*

Abstract

In this paper, the analysis of the local exergy costs of a cullet glass heated by microwaves in a cubical cavity activated by a susceptor is presented. The analysis is based on a previously validated 3-D electromagnetic model, but goes further by applying the concepts of local exergy efficiency and local unit exergy consumption, what enables a local analysis (in time and space) of the process efficiency. Furthermore, local exergy cost quantifies in detail the path of the exergy cost formation during microwave heating, which is determined by the local irreversibilities taking place in this transient process.

Four different susceptor positions have been also compared, in order to find out not only which one is the most efficient but also to justify in detail this result by the time and space evolution of efficiency, unit exergy consumption (both external microwave power and conduction contributions) and unit exergy cost. The best conclusion of the paper is that the local exergy cost approach can contribute to the design of more efficient energy conversion systems, as it could be noted in its application to a complex process like this 3-D example of microwave cullet heating.

Keywords:

Microwave heating, cullet glass, susceptor, exergy transfer, local exergy efficiency, local exergy cost.

1. Introduction

The aim of exergy analysis is to improve energy efficiency and to achieve a rational use of natural resources. It is based on the Second Law of Thermodynamics through the concept of exergy, that is, the maximum work that a system or flow could perform while interacting with the environment or, alternatively, the minimum work necessary to develop the inverse process. This magnitude has the advantage of taking into account not only energy quantity but also energy quality, and therefore enables to identify and quantify where irreversibility occurs or, in other words, where inefficiencies take place. Several detailed examples of exergy analysis can be seen, for instance, in the work of Szargut [1], Kotas [2] or Dincer and Çengel [3].

It is possible to go a step further by introducing the concept of purpose, what allows one to classify flows within a system component into product (i.e. flows related to the purpose of the system) and fuel (resources consumed for obtaining that product). The quotient between product and fuel is the component efficiency, and its inverse is the component unit exergy consumption. In this sense, the concept of a cost associated to the irreversibility was firstly introduced by Tribus and Evans [4], who coined the term Termoeconomics for the combination of Thermodynamics (exergy analysis) and Economics (the concept of cost). Thus, the exergy cost of a flow within a system is the amount of exergy resources entering the system that are needed to produce that flow, whereas unit exergy cost is the quotient between exergy cost and exergy. Thus, the chain of the cost formation process along the

consecutive processes in a complex system could be accounted for. If monetary costs are introduced, exergoeconomic costs are obtained. Details about thermoeconomic analysis are presented in the papers by Szargut [1], Lozano and Valero [5,6], Torres [7] or Tsatsaronis [8], among others.

Although exergy and thermoeconomic analyses are usually focused on thermal and chemical systems, the number of applications to systems where electricity plays a relevant role is growing. Exergy analysis of several electric devices, in particular, the electromagnet, was reported by Rosen and Bulucea [9,10]. Plasma systems were analyzed from the exergy perspective by Petela and Piotrowicz [11]. In [12], Ranjbaran and Zare presented the exergy analysis of a microwave drying system.

Sometimes, exergy and thermoeconomic analyses are combined with other advanced techniques, such as neural networks. For instance, in [13] exergy and energy were applied for the calculation of heating cost in a district heating net that had been modeled by neural networks. A model of the control of a combined heat and power plant based on artificial neural networks, fuzzy logic and exergy is presented in [14].

In most cases, exergy analysis is applied at component level or, in other words, as a black-box approach and also at steady state. Sometimes, the transient nature of the process has to be considered, such as in the temporal exergy analysis of adsorption cooling system developed by Sharifzadeh et al. [15] or for unsteady heat conduction [16]. However, it is also interesting to analyze processes at microscopic level by quantifying space and time dependence of exergy transformations. Regarding exergy transfer, and as it is explained by Qing-lin and Yao [17], the transition from exergy to exergy transfer should be as natural as the transition from heat to heat transfer. In [18], Soma first presented a 1-D exergy transfer equation. Then, a two dimensional conduction example was analyzed by Chun-Zhen et al. [19]. In [20], Lior et al. presented a detailed review of the methodology. Recently, exergy transfer has been extensively used to optimize forced convective heat transfer in ducts [21,22] or tubes [23-25], sometimes alternatively using the local exergy destruction minimization. Porous media [26], surfactant solutions [27], heat exchanger effectiveness [28] or counter flow wet cooling towers [29] have been also studied in depth by the exergy transfer analysis. Finally, it is noteworthy the concept of an exergy transfer coefficient connected to the Nusselt and Reynolds numbers to improve the internal thermodynamic efficiency of a sinter bed layer [30,31].

While exergy transfer locally describes the changes of the energy quality during the heat transfer process, the use of local exergy cost balance permits to go a step further by showing the history of the process efficiency, that is, the cumulative costs from the beginning to the end of that process. In [32], the local exergy cost theory was firstly presented by Rangel et al. and it was shown how this local analysis can provide useful information about where exergy is destroyed and the cost caused by this irreversibility. However, the first attempt to develop this local exergy cost can be found in [33,34], where Wang et al. introduced the development of the exergy cost transfer equation. If transient analysis including exergy costs is finally tested, thermal storage systems are usually the most unsteady process in complex systems, and two approaches can be found in the literature, the first joined to the local entropy generation [35] or the hourly cost allocation in trigeneration systems [36].

Regarding microwaves heating process, it has been verified as an effective but complex method, thus becoming an emerging research field. For instance, Santos et al. developed a microwave heating model of a ceramic sample [37]. Mishra and Sharma analyzed the in-situ microwave heating of bulk Al-7039 alloy [38]. Hong et al. presented a 3-D simulation of microwave heating of a coal sample [39]. Since microwave heating is a volumetric process, it is suitable to perform a local exergy analysis. A general equation of the exergy balance with its exergy local cost to this process was firstly presented by Acevedo et al. in [40,41]. A complete description of a simple 2-D exergy transfer field and their associated local exergy costs were presented for two different heating methods applied to a potato slice: microwave and

conventional oven (by convection). This was a preliminary example in which heat generation due to microwaves was calculated by using the Lambert's Law. Such simplification was very useful for showing the main concepts of that new approach, but a realistic 3-D case is required for demonstrating its complete applicability in real microwave heating processes.

Accordingly, the aim of the present work is to apply the local exergy cost methodology introduced in [41] to a 3-D realistic case study: the analysis of microwave heating of cullet glass activated with a susceptor, including the sensitivity analysis of its location. This 3-D model was already validated in that paper with existing literature, and temperature deviations were really low. In the first part of this paper, the formulation of the methodology of local exergy cost is presented for a 3-D microwave heating case. Then, the example is described and results of the base case are presented: local exergy efficiency, local unit exergy consumption and local unit exergy cost. Finally, the effect of susceptor position on the aforementioned parameters is analyzed. Calculations are based on system modeling and exergy transfer analyses developed by the authors [42,43].

Results show in detail how local exergy-related parameters vary along space and time inside of the glass during the heating process. First of all, local exergy efficiency is calculated for all points during the whole heating process. This parameter is the quotient between local exergy increment due to heating (useful effect) and exergy provided by both microwaves and heat conduction. Areas with low exergy efficiency should be avoided or, at least, reduced; accordingly, its detection shows potential for system design improvement. Local unit exergy consumption is the inverse of local exergy efficiency (and, thus, provides the same information) but has an additional advantage because it can be decomposed into the summation of two terms: one due to the contribution of microwaves and other due to exergy transfer by conduction; accordingly, it allows one to analyze in detail how both resources are used for the purpose of cullet glass heating. Finally, local exergy costs were computed in order to fully understand the cost formation process along the system. Local unit exergy cost accounts for the amount of exergy entering the system consumed for obtaining a unit of exergy of useful effect (glass heating). Accordingly, this parameter quantifies for each point and for each time how efficient has been the whole process of heating of that point till that time (in other words, the history of the heating process). A point with high unit exergy cost shows that its heating process has been inefficient, whereas a point with low unit exergy cost indicates that its heating has been efficient.

As a result of the analysis, points with high local exergy cost and/or low exergy efficiencies are identified ('hot spots'), being the first information to improve the system design (by modifying the design in order to reduce these points).

As far as the authors' knowledge, it is the first combined approach of using local exergy transfer and exergy costs in such complex heating process (3D model of microwave glass heating including a susceptor). It is worth to emphasize again that local exergy cost analysis (LEC) complements exergy transfer analysis (ET) in order to finally achieve all the objectives pointed out in [20] for the exergy analysis. This is summarized in Table 1 and specifically adapted for microwave heating of cullet glass included in this paper.

Analysis:	Objective achieved by:
Identification of irreversibilities	*Irreversibility calculation (ET)*
Understanding why losses occur	*Exergy flows and rate change of exergy (ET)*
Evaluation of changes, parameters and configurations	*Analysis of different susceptor locations (ET, LEC)*
Suggestions on improvements	*Exergy destruction (ET)*
	Local exergy efficiency, local unit exergy consumption (LEC)
Accounting for the effects of losses and assessing a final cost to the product	*Local exergy cost (LEC)*

Table 1. Summary of how objectives proposed in [20] are achieved by exergy transfer (ET) and local exergy cost (LEC).

2. From global to local Thermoeconomic analysis

The aim of this section is to present the methodology of local exergy and exergy cost analyses. First, concepts of exergy efficiency and unit exergy consumption are summarized for the classical macroscopic analysis applied to systems formed by several components. Then, these ideas are extended to local analysis. Afterwards, the idea of exergy cost for exergy flows (macroscopic analysis) is outlined. Finally, calculation of local exergy cost is introduced.

2.1 Exergy efficiency and unit exergy consumption in macroscopic analysis

When a system is analyzed from a macroscopic perspective, Exergy Cost Theory provides a general methodology to assess the exergy efficiency and rationally explain the cost formation process of the products in a system [5,6]. To accomplish that goal, the definition of fuel and product for each component is needed, both in terms of exergy. Fuel represents resources consumed by the component whereas product refers to the useful effect that this component has. Ideally, all fuel would be transformed into product. However, in a real process irreversibilities occur, thereby producing exergy losses.

$$\dot{\mathrm{F}} - \dot{\mathrm{P}} = \dot{\mathrm{I}} \geq 0 \qquad (1)$$

In the previous equation, F is fuel, P is product and I, according to the Guy-Stodola Theorem, quantifies in terms of exergy destruction the process irreversibility [6]. This means that, since the system is a real process, the quality degradation in the system can be measured by the definition of products and fuels. To this end, it is defined the concept of exergy efficiency which represents a universal ratio to evaluate thermodynamic quality of that process:

$$\eta_{\mathrm{b}} = \dot{\mathrm{P}} \Big/ \dot{\mathrm{F}} \leq 1 \qquad (2)$$

The inverse of Eq. (2) represents the unit exergy consumption of a component, which quantifies the amount of exergy units that each component consumes to obtain a unit of its product.

$$\kappa_{\mathrm{b}} = \dot{\mathrm{F}} \Big/ \dot{\mathrm{P}} = 1 \Big/ \eta_{\mathrm{b}} \geq 1 \qquad (3)$$

where k_b is unit exergy consumption of the component.

2.2 Local efficiency and local unit exergy consumption

The first step to define local efficiency and unit exergy consumption is to consider the exergy transfer equation. For a solid with a constant density and thermal conductivity affected by microwaves, this equation is [43]:

$$\nabla\cdot\left[k\nabla T\left(1-\frac{T_0}{T}\right)\right]+\dot{b}_{MW}=\rho\frac{da}{dt}+\dot{b}_D \quad (4)$$

In left side of Eq. (4), the first term quantifies the exergy transfer due to heat conduction (heat conduction flow times the Carnot factor) whereas the second term is the exergy rate entering the differential volume by microwaves $\dot{b}_{MW}$. On the right side, first term quantifies the exergy accumulation and the second represents destroyed exergy rate. In other words, equation **(4)** states that exergy can be gained by conduction and microwaves and, then, can be accumulated or destroyed. Accordingly, fuel is composed of exergy transfer by heat conduction and exergy provided by microwaves, and product is the exergy accumulation. With this information and taking in to account that the main purpose is to heat up the system (exergy accumulation), the productive purpose of each term can be defined as [41]:

Equation term	Purpose	Definition
Exergy of heat conduction $\nabla\cdot\left[k\nabla T\left(1-\frac{T_0}{T}\right)\right]$	*Exergy balance of inputs and outputs flows through the element.*	*Fuel*
Exergy of volumetric heat generation $\dot{b}_{MW}$	*Exergy input due to microwaves.*	*Fuel*
Exergy accumulation $\rho\frac{da}{dt}$	*Final exergy gained by differential volume.*	*Product*
Destroyed exergy $\dot{b}_D$	*Loss of energy quality.*	*Irreversibility*

Table 2. Productive definition of a differential volume in microwave heating [41]:

According to the aforementioned fuel-product definition and to Eq. (4), the local efficiency of the exergy transfer process is defined as:

$$\eta_{b(x,y,z,t)}=\frac{\rho\frac{da}{dt}}{\nabla\cdot\left[k\nabla T\left(1-\frac{T_0}{T}\right)\right]+\dot{b}_{MW}} \quad (5)$$

Therefore, the unit exergy consumption has two contributions: heat conduction exergy (κ_Q) and volumetric exergy input of microwaves (κ_{MW}):

$$\kappa_{b(x,y,z,t)}=\kappa_{Q(x,y,z,t)}+\kappa_{MW(x,y,z,t)} \quad (6)$$

Where:

$$\kappa_{Q(x,y,z,t)} = \frac{\nabla \cdot \left[k \nabla T \left(1 - \frac{T_0}{T} \right) \right]}{\rho \frac{da}{dt}} \quad (7)$$

$$\kappa_{MW(x,y,z,t)} = \frac{\dot{b}_{MW}}{\rho \frac{da}{dt}} \quad (8)$$

It is convenient to present the discretized version of the previous equations. The general 3-D exergy transfer rate balance of a finite volume for a point with coordinates (i,j,k) at a time step n is [43]:

$$\dot{B}^n_{(i+1,j,k)} + \dot{B}^n_{(i-1,j,k)} + \dot{B}^n_{(i,j+1,k)} + \dot{B}^n_{(i,j-1,k)} + \dot{B}^n_{(i,j,k+1)} + \dot{B}^n_{(i,j,k-1)} + \dot{B}^n_{MW(i,j,k)} = \left(\frac{dA}{dt} \right)^n_{(i,j,k)} + \dot{B}^n_{D(i,j,k)} \quad (9)$$

Terms of the exergy balance presented in Eq. (9) are described as follows:

- The first six terms correspond to exergy flows entering the control volume due to conduction heat transfer. For instance, the first term $\dot{B}_{(i+1,j,k)}$ for an inner node is calculated as:

$$\dot{B}^n_{(i+1,j,k)} = \Delta y \cdot \Delta z \cdot k \left(\frac{T_{(i+1,j,k)} - T_{(i,j,k)}}{\Delta x} \right) \left(1 - \frac{2T_0}{T_{(i,j,k)} + T_{(i+1,j,k)}} \right) \quad (10)$$

  Note that these terms should also contain the radiative effect when it is relevant (e.g. in the glass boundary and susceptor) as it was detailed in [43].
- $\dot{B}_{MW}$: Exergy from microwaves.

$$\dot{B}^n_{MW(i,j,k)} = \Delta x \cdot \Delta y \cdot \Delta z \cdot \dot{q}_{MW(i,j,k)} \quad (11)$$

- $(dA/dt)^n_{(i,j,k)}$: Change on internal exergy.

$$\left(\frac{dA}{dt} \right)^n_{(i,j,k)} \cong \frac{\Delta x \cdot \Delta y \cdot \Delta z \cdot \rho \cdot c \left[\left(T^n_{(i,j,k)} - T^{n-1}_{(i,j,k)} \right) + T_0 \ln \left(\frac{T^{n-1}_{(i,j,k)}}{T^n_{(i,j,k)}} \right) \right]}{\Delta t} \quad (12)$$

- $\dot{B}^n_D$: Destroyed exergy. It is calculated by difference in eq. 9.

It should be highlighted that the methodology is applied after solving the electromagnetic/thermal model previously validated in [42]. Accordingly, the values of temperatures and energy flows are already known. Fig. 1 shows a graphic representation of these terms.

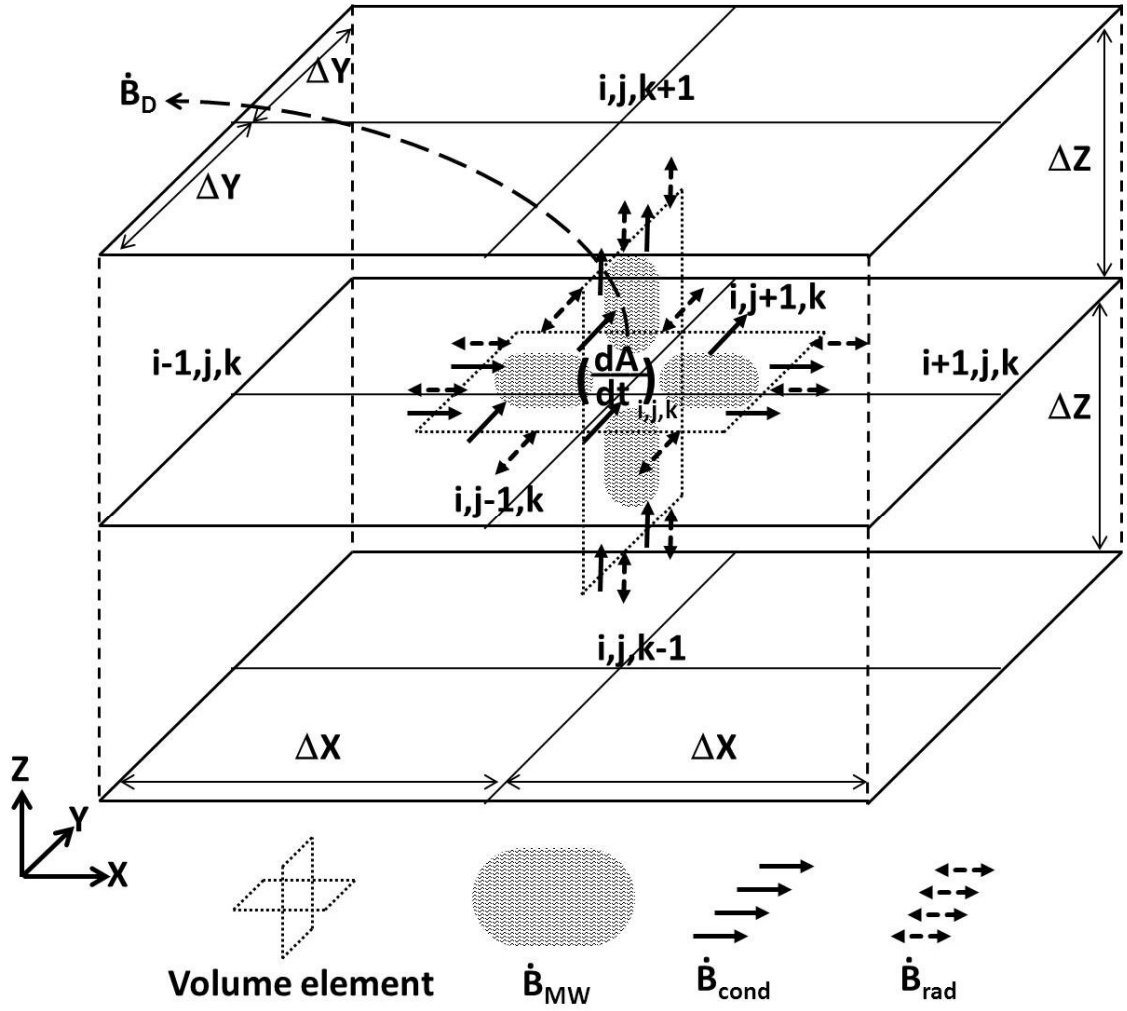

Fig. 1 Exergy transfer: general balance for a generic 3-D cell.

Local efficiency (eq. 5) is discretized as:

$$\eta^{n}_{b(i,j,k)} = \frac{\left(\frac{dA}{dt}\right)^{n}_{(i,j,k)}}{\dot{B}^{n}_{(i+1,j,k)} + \dot{B}^{n}_{(i-1,j,k)} + \dot{B}^{n}_{(i,j+1,k)} + \dot{B}^{n}_{(i,j-1,k)} + \dot{B}^{n}_{(i,j,k+1)} + \dot{B}^{n}_{(i,j,k-1)} + \dot{B}^{n}_{MW(i,j,k)}} \quad (13)$$

Besides, the discretized forms of (eqs. 6 to 8) allow the calculation of local unit exergy consumption, taking into account the effects of heat conduction (κ_Q) and microwaves (κ_{MW}):

$$\kappa^{n}_{b(i,j,k)} = \kappa^{n}_{Q(i,j,k)} + \kappa^{n}_{MW(i,j,k)} \quad (14)$$

$$\kappa^{n}_{Q(i,j,k)} = \frac{\dot{B}^{n}_{(i+1,j,k)} + \dot{B}^{n}_{(i-1,j,k)} + \dot{B}^{n}_{(i,j+1,k)} + \dot{B}^{n}_{(i,j-1,k)} + \dot{B}^{n}_{(i,j,k+1)} + \dot{B}^{n}_{(i,j,k-1)}}{\left(\frac{dA}{dt}\right)^{n}_{(i,j,k)}} \quad (15)$$

$$\kappa^{n}_{MW(i,j,k)} = \frac{\dot{B}^{n}_{MW(i,j,k)}}{\left(\frac{dA}{dt}\right)^{n}_{(i,j,k)}} \quad (16)$$

2.3 Exergy cost in macroscopic analysis

In a macroscopic level at steady state, the exergy cost $\dot{B}^*$ of an exergy flow $\dot{B}$ within a system is the amount of exergy per time unit entering the system to create that flow [5]. Exergy cost is, thus, a conservative property related to the productive process (taking into account all the irreversibilities generated within the analyzed system for producing the flow). The corresponding definition of exergy cost is:

$$\dot{B}^{*} = \dot{B} + \sum \dot{I} \quad (17)$$

Where $\dot{I}$ corresponds to the irreversibilities generated during the production of the given flow. The unit exergy cost k^* of a flow is the ratio between its exergy cost and its exergy as shown in Eq. (18):

$$k^{*} = \dot{B}^{*} \Big/ \dot{B} \quad (18)$$

2.4 Local exergy cost

In local analysis and batch processes like melting glass, the use of specific non-flow exergy a is recommended instead of exergy flows ($\dot{B}$) [32,41]. Accordingly, local unit exergy cost is defined as:

$$k^{*} = \frac{a^{*}}{a} \quad (19)$$

In Eq. (19) a is the specific non-flow exergy and a^* is its respective exergy cost, both in J/kg. Then, differential local exergy cost equation for a solid with constant density and thermal conductivity, in transient state and with volumetric heat generation has the form [41]:

$$\nabla \cdot \left[k^{*}_{b} k \nabla T \left(1 - \frac{T_0}{T} \right) \right] + k^{*}_{e} \dot{b}_{MW} = \rho \frac{d\left(k^{*}_{a} a\right)}{dt} \quad (20)$$

Complete development of Eq. (20) can be found in [32-34,41]. The previous equation shows how the exergy cost transferred by heat conduction (first term of left side) plus the exergy cost due to microwaves (second term of left hand side) has to be equal to the cost of exergy accumulation (right side term). Accordingly, k^*_b is the unit exergy cost of the exergy

transferred by heat conduction, k_e^* is the unit exergy cost of of external source (microwaves) and k_a^* is the unit exergy cost of the accumulated exergy.

In order to apply the previous cost balance to a numerically modeled system, the 3-D balance of the exergy cost should be discretized as:

$$\left(\begin{matrix}\mathrm{k}^{*n}_{b(i+1,j,k)}\dot{\mathrm{B}}^{n}_{(i+1,j,k)}+\mathrm{k}^{*n}_{b(i-1,j,k)}\dot{\mathrm{B}}^{n}_{(i-1,j,k)}+\mathrm{k}^{*n}_{b(i,j+1,k)}\dot{\mathrm{B}}^{n}_{(i,j+1,k)}+\\ +\mathrm{k}^{*n}_{b(i,j-1,k)}\dot{\mathrm{B}}^{n}_{(i,j-1,k)}+\mathrm{k}^{*n}_{b(i,j,k+1)}\dot{\mathrm{B}}^{n}_{(i,j,k+1)}+\mathrm{k}^{*n}_{b(i,j,k-1)}\dot{\mathrm{B}}^{n}_{(i,j,k-1)}\end{matrix}\right)+\mathrm{k}^{*n}_{e}\dot{\mathrm{B}}^{n}_{MW(i,j,k)}=\frac{\left(\mathrm{A}^{n+1}_{(i,j,k)}\mathrm{k}^{*n+1}_{a(i,j,k)}\right)-\left(\mathrm{A}^{n}_{(i,j,k)}\mathrm{k}^{*n}_{a(i,j,k)}\right)}{\Delta t} \quad \textbf{(21)}$$

In left side, the first six terms represent the exergy cost transferred by heat conduction, and the last term corresponds to the exergy cost of microwaves. Right side term indicates the cost of the exergy accumulation in the discretized volume.

It should be emphasized that an additional condition is required in order to close the cost balance, since two cost sources are entering in the heated glass. This condition is related to the unit exergy cost of heat flows k_b^* and microwaves k_e^*. Two different approaches were presented and analyzed in [41] for the case of microwave heating:

- **Input/output approach**: Unit exergy cost of each conduction exergy transfer flow ($k^{*n}_{b(i,j,k)}$) is equal to the unit exergy cost of the exergy accumulated in the differential volume where it comes from ($k^{*n}_{a(i,j,k)}$).

$$\mathrm{k}^{*n}_{b(i,j,k)}=\mathrm{k}^{*n}_{a(i,j,k)} \quad \textbf{(22)}$$

- **Fuel/product approach:** Unit exergy cost of each conduction exergy transfer flow ($k^{*n}_{b(i,j,k)}$) is equal to the unit exergy cost of the external source (fuel) that generates the exergy transfer process, which is the microwaves exergy (k_e^{*n}).

$$\mathrm{k}^{*n}_{b(i,j,k)}=\mathrm{k}^{*n}_{e} \quad \textbf{(23)}$$

In the example analyzed in [41], this cost was constant along the whole process. In other words, according to that approach, the fuel of the heating process is the exergy coming from microwaves minus the exergy transferred by conduction to other cells; for this reason, they have the same unit exergy cost. Thus, the fuel-product approach has been also applied to melting cullet glass according to these observations:

- Microwaves are the only heating source used during the heating and further melting.
- At the beginning of the heating process, all the increment of the susceptor exergy comes from microwaves. Therefore, the exergy used to perform glass activation comes from those microwaves.
- The magnitude of the exergy transfer generated by heat conduction is always smaller than the one produced by microwaves (see [42,43] for details).
    - During cullet activation stage, internal exergy flows are only created by microwaves. Exergy transfer produced by heat conduction is almost negligible.
    - After the cullet activation, the exergy transfer by heat conduction is smaller but of similar order of magnitude as the one produced by microwaves.

Nevertheless, in [41] both approaches were applied to a simple 2-D example by using two heating technologies: conventional oven and microwaves. In conventional heating, when input-output approach was applied, the unit exergy cost of the heating was moved along the

heating piece at the same rate as temperature was increased, whereas when the fuel-product approach was used, the unit exergy cost of heating was concentrated in the place where the heating source was applied. However, with microwave heating most of the time the microwaves exergy was higher than the exergy transfer by internal conduction, both approaches produced rather similar results in their local exergy costs.

When the fuel-product approach is applied, as the unit exergy cost of flows $k^{*n}_{b(i,j,k)}$ is associated to the unit exergy cost of the microwaves k^{*n}_{e} that generates the exergy transfer process, equation (21) could be rewritten as:

$$k^{*n+1}_{a(i,j,k)} = \frac{\left[\begin{pmatrix} k^{*n}_{e}\dot{B}^{n}_{(i+1,j,k)} + k^{*n}_{e}\dot{B}^{n}_{(i-1,j,k)} + k^{*n}_{e}\dot{B}^{n}_{(i,j+1,k)} + \dots \\ k^{*n}_{e}\dot{B}^{n}_{(i,j-1,k)} + k^{*n}_{e}\dot{B}^{n}_{(i,j,k+1)} + k^{*n}_{e}\dot{B}^{n}_{(i,j,k-1)} \end{pmatrix} + k^{*n}_{e}\dot{B}^{n}_{MW(i,j,k)}\right]\Delta t + A^{n}_{(i,j,k)}k^{*n}_{a(i,j,k)}}{A^{n+1}_{(i,j,k)}} \quad \textbf{(24)}$$

In other words, equation (24) states that the unit exergy cost of the differential volume $a_{(i,j,k)}$ does not directly depend on the unit exergy costs of their surroundings. The main exergy input increasing the unit exergy cost $k^{*}_{a(i,j,k)}$ is the volumetric generation $\dot{B}_{MW}$ with its corresponding unit exergy cost k^{*}_{e}. With this equation, the evaluation of the local unit exergy cost during microwave cullet heating can be performed as represented in Figure 2.

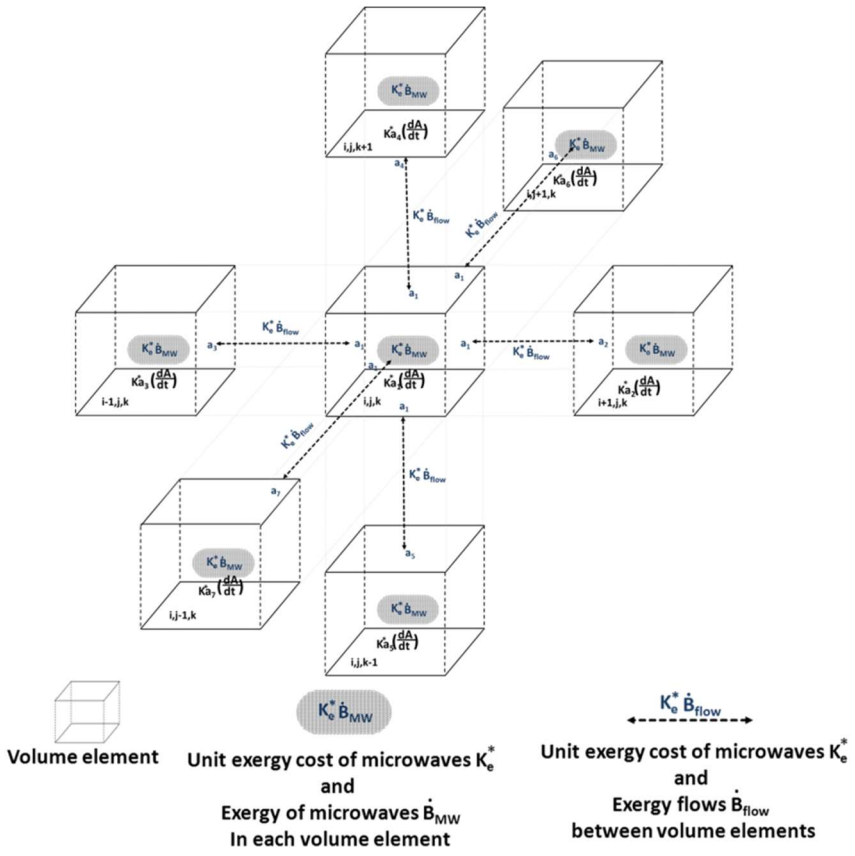

Fig. 2 Local exergy cost (Glass melting case).

3. Case study: cullet glass heating activated by SiC susceptor (base case)

The methodology presented above has been applied to a microwave system to melt cullet glass. Since at temperatures below 300 °C glass is transparent to microwave radiation, a

silicon carbide (SiC) susceptor has to be immersed in the applicator to start heating: the susceptor is first heated by microwaves and then glass in contact is heated by conduction. When glass reaches a temperature of around 300 °C dielectric properties allow one to absorb the microwave radiation: this process is called activation.

Fig. 3 shows the microwave system configuration, which includes four different susceptor positions (A to D) and two studied points (P1 and P2). Table 3 shows the system dimensions: applicator, cavity, waveguide and susceptor (including its relative location).

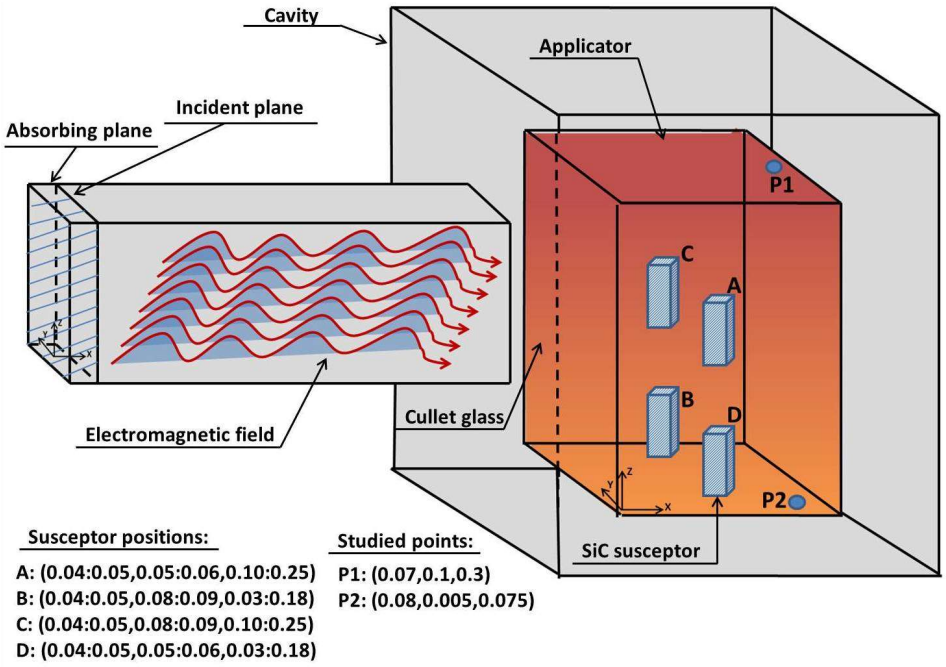

Fig. 3 Microwave system to melt glass.

Unit	Dimensions [m]
Applicator	0.09 x 0.1 x 0.3
Cavity	0.25 x 0.25 x 0.43
Susceptor	0.01 x 0.01 x 0.15
Waveguide	
Length	0.3
Width	0.2
Height	0.35

Table 3 Microwave system main dimensions.

A mathematical model of the heating process was described and developed in [42]. As explained in that paper, model was validated by adapting the case and comparing results with those obtained in the literature. Besides, diverse temperature profiles were obtained depending on the susceptor location. The model is based on transient Maxwell's equations solved by a finite difference time domain (FDTD) method in 3-D. Furthermore, heat conduction along the glass was computed by applying an effective thermal conductivity coefficient that

takes into account both real conduction and an equivalent term due to radiation (see [42] for details). Accordingly, it is much more complex and accurate than the simplified 1-D approach of Lambert's Law applied in the previous application of local exergy cost to microwave heating systems [40,41]. Then, in [43], exergy transfer analysis was applied to this case study. It should be noted that exergy transfer terms are calculated by using only results from the validated model; accordingly, no additional validation is needed neither for exergy transfer nor for exergy cost analyses. Finally, in this paper, local exergy efficiency, local unit exergy consumption and local exergy cost have been estimated by applying the formulation presented in the previous section. As a result, the degradation cost path of exergy resources consumed along the whole heating process can be observed in detail. Accordingly, this analysis allows a better interpretation of the process and can provide useful information for detecting potentials of energy savings, in the sense of trying to avoid those points with low local exergy efficiency and/or long low-efficient heating periods.

Four different susceptor positions have been proposed; in this section, a base case (case A) is analyzed and in section 4 three new positions (cases B to D) have been added and compared by means of the local exergy cost analysis.

3.1 Local exergy efficiency

Local efficiency of the microwave heating process has been computed by applying Eq. (13) and appears in Fig. 4 and Fig. 5 for the base case (susceptor in position A) and at the times of 1, 10, 20 and 36 minutes.

At the beginning, when glass is not yet activated, exergy activity appears only within the susceptor. After one minute the susceptor center presented an exergy efficiency about 65%. However, in the zone in contact with the glass, susceptor efficiency was only about 35%. On the other hand, the cullet glass surrounding the susceptor has an efficiency of 50%, due to the activation process (heating by conduction). The glass far from the susceptor is also subjected to the microwaves field, but the absorption is very poor, for that reason the efficiency is almost 0%. It should be noted that the efficiency depends not only on the ability of absorbing microwave energy, but also on temperature: at higher temperatures, the heating process is less irreversible and consequently efficiency increases.

After the complete activation (minute 10), the glass became a fully absorbent material to the applied microwaves field, what produces a high amount of interaction between the exergy fuels (microwaves and exergy transfer flows) and the increment of non-flow internal exergy. Besides, temperature increased and, thus, irreversibility in microwave heating decreased. Therefore, highly efficient areas appeared in the whole glass volume and not only in the immediate vicinity of the susceptor. On the contrary, from now to the end the efficiency of the susceptor was very low compared with the cullet. This effect appears because susceptor had reached a quite high temperature, and the rate of increment of this temperature decreased, what causes that the rate of increment of exergy also decreased.

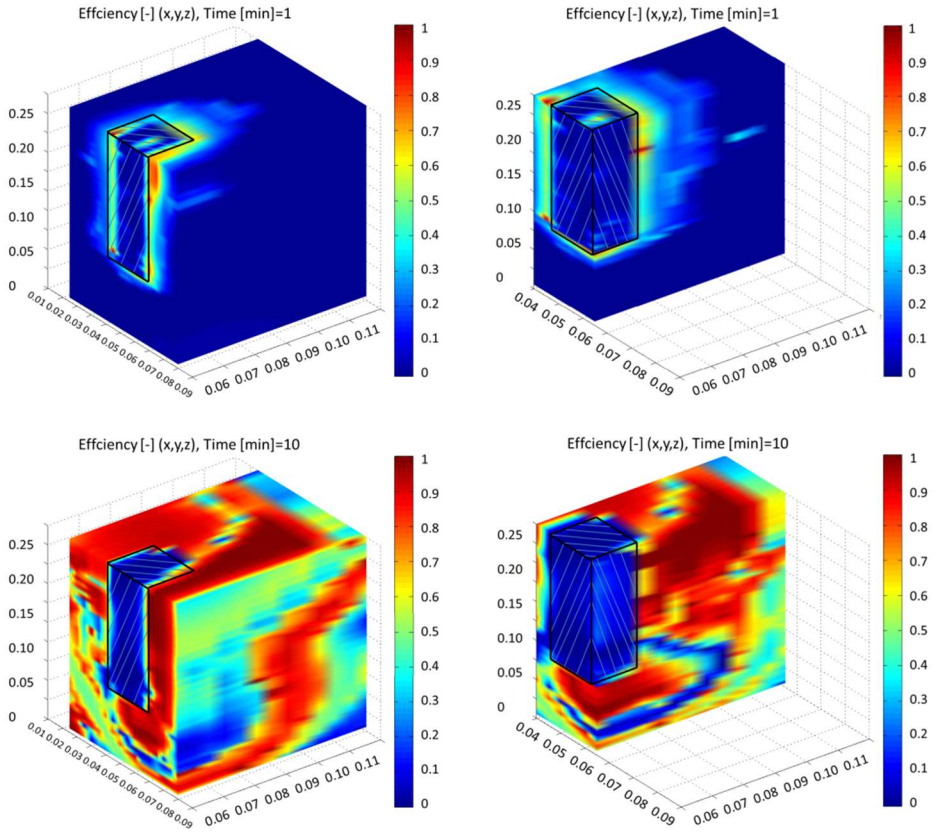

Fig. 4 Local exergy efficiency at minutes 1 and 10.

After 20 minutes of simulation, most of the microwave energy is absorbed by glass cullet as described in [44,45], since the absorption ability (or effective loss factor ε'') increases almost exponentially at temperatures above 300 °C. It can be observed that the local efficiency increases as temperature rises and then in turn induces important changes on the dielectric properties of glass, mainly the effective loss factor. By the end of the simulation (36 minutes), internal parts remain at high level of exergy efficiency (above 80%) while in the edges those indexes decrease (to around 20%).

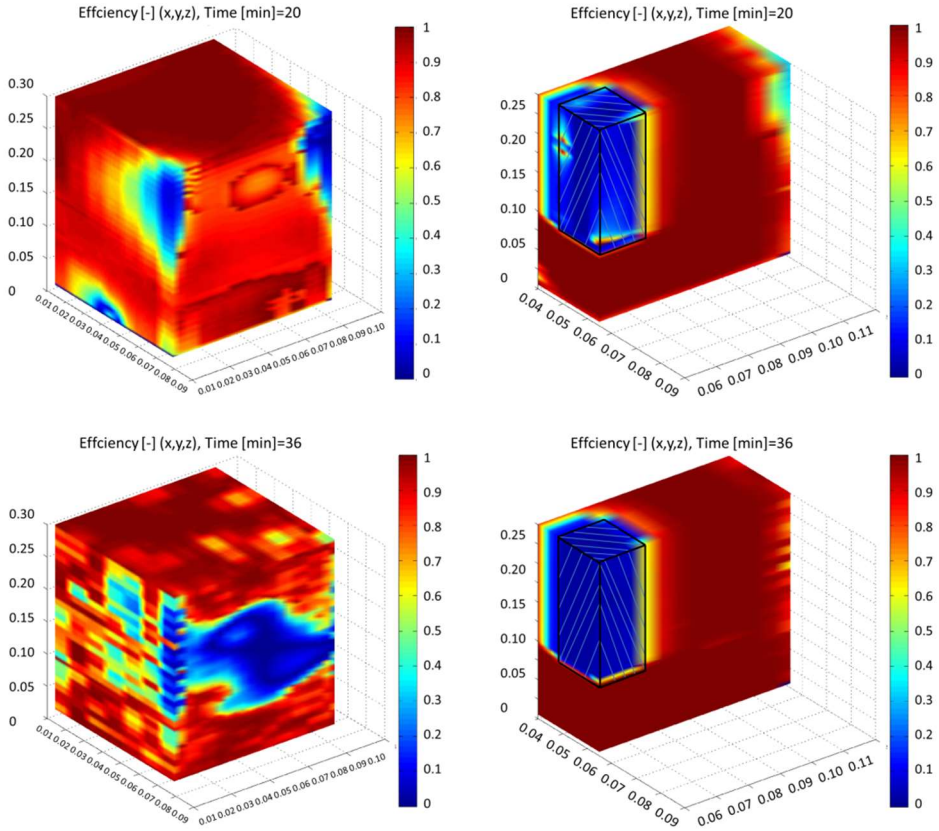

Fig. 5 Local exergy efficiency at minutes 20 and 36.

3.2 Local unit exergy consumption

The local unit exergy consumption is the inverse of efficiency but it can separately describe the contributions of both exergy sources within the cullet glass: microwave and heat conduction (see Eq. 6 and 14). Fig. 6 and Fig. 7 show the local unit exergy consumption: on the left side the microwave contribution (k_{MW}) and on the right side the one provoked by heat conduction (k_Q).

In Fig. 6, it can be observed that at the beginning of the simulation the activation is performed due to the exergy flows caused by heat transfer between susceptor and glass. As cullet glass is under the effects of a microwave field but the activation is not performed yet, the local unit exergy consumption by microwaves is very high; in these points, high quality energy of microwaves is transformed into very low quality energy (heating slightly above ambient temperature). In the case of heating by heat conduction, unit exergy consumption is not so high in the susceptor area since the reduction of energy quality is lower (from medium temperature to low temperature), but higher values in the farther areas to the susceptor can be found (because of their low temperature). By the minute 10, local unit exergy consumption considerably decreases, and the highest values appear inside of the susceptor that continuously exchanges exergy with the surrounding cullet glass. This effect corresponds to the lower efficiency observed in that area.

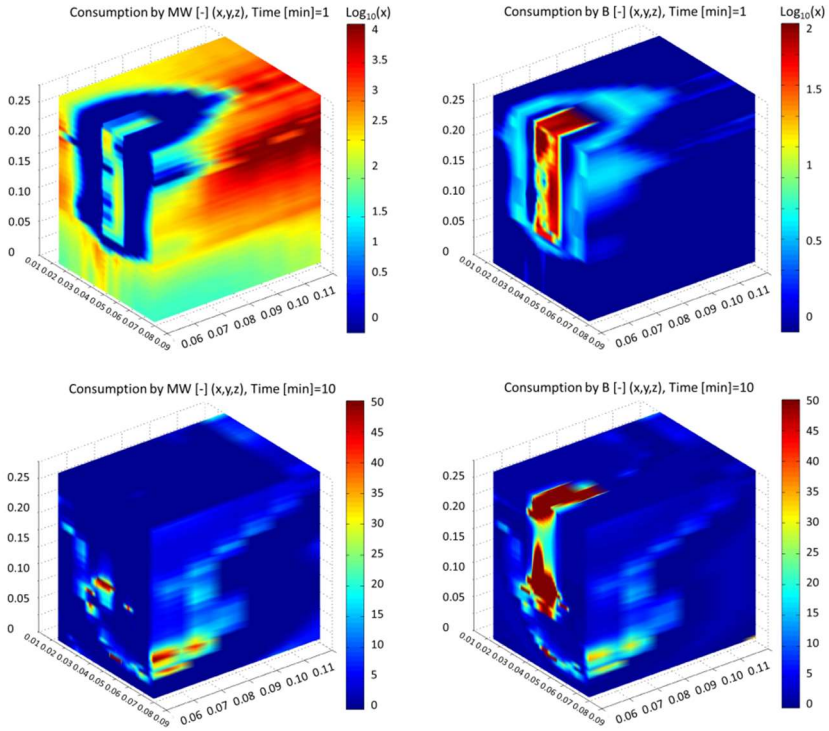

Fig. 6 Local unit exergy consumption at minutes 1 and 10 (left: microwave contribution, right: heat conduction flows contribution)

Fig. 7 shows that at the end of the simulation the local unit exergy consumption (microwave and conduction flows contributions) decreased, which means that the process is more efficient. At minutes 20 and 36 glass was fully activated at cullet temperatures above 300 °C, but heat transfer also contributed to the heating process. Furthermore, and due to higher operating temperatures, the irreversibility of both heating methods decreased. As a result, both terms of unit exergy consumption have the same order of magnitude. Besides, it can be seen how at the end of the process higher values of unit exergy consumption are concentrated in the edges.

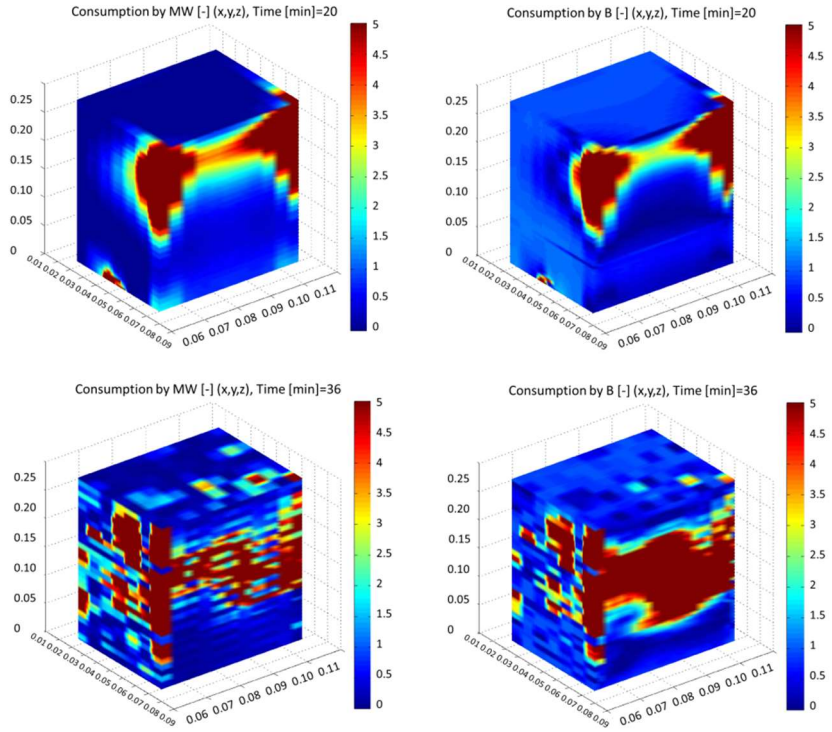

Fig. 7 Local unit exergy consumption at minutes 20 and 36 (left: microwave contribution, right: heat conduction flows contribution).

3.3 Local unit exergy cost

In this section, the evolution of the local unit exergy cost during the heating process is analyzed. As it was explained previously, this cost represents the amount of exergy coming from external resources needed for producing a unit of exergy in the cullet glass. In other words, this magnitude quantifies the accumulated exergy efficiency along the 'history' of the heating process: the lower that 'aggregated' efficiency, the higher the unit exergy cost.

The local unit exergy cost in the cullet glass and susceptor has been computed by using Eq. (24). It has been considered that microwaves are generated with electrical power having a global efficiency of 85% in the microwave generator [40]. Thus, the unit exergy cost of the microwave exergy received in the cullet glass and susceptor is the inverse of that value; in other words, the value of k_e in Eq. (24) is equal to 1/0.85=1.1764.

In Fig. 8, it can be seen that at minute one the cost of glass is about 30 units in the areas nearby the susceptor. However, this cost was incremented to values about 10000 units in remote areas close to cullet ends. The cost in susceptor is around 100 units. These differences in unit exergy cost are produced by the effective loss factor of the cullet glass and the magnitude of the exergy transferred inside of the glass, as well as the temperature of the heated points. Below 300 °C, glass was unable to convert microwave energy into heat. Around the susceptor, glass incremented its temperature but not enough to do it efficiently as explained before. The low temperature of the points located away from the susceptor makes their heating very inefficient, what causes the high cost values. However, at 10 minutes glass was fully activated and the local cost was considerably reduced except in the susceptor zone. Due to the irreversibility of the conversion from high quality microwave energy to low-grade thermal energy, local exergy cost in some susceptor areas remains in values around 70 units during the whole process, as it can be seen in Fig. 8 and Fig. 9.

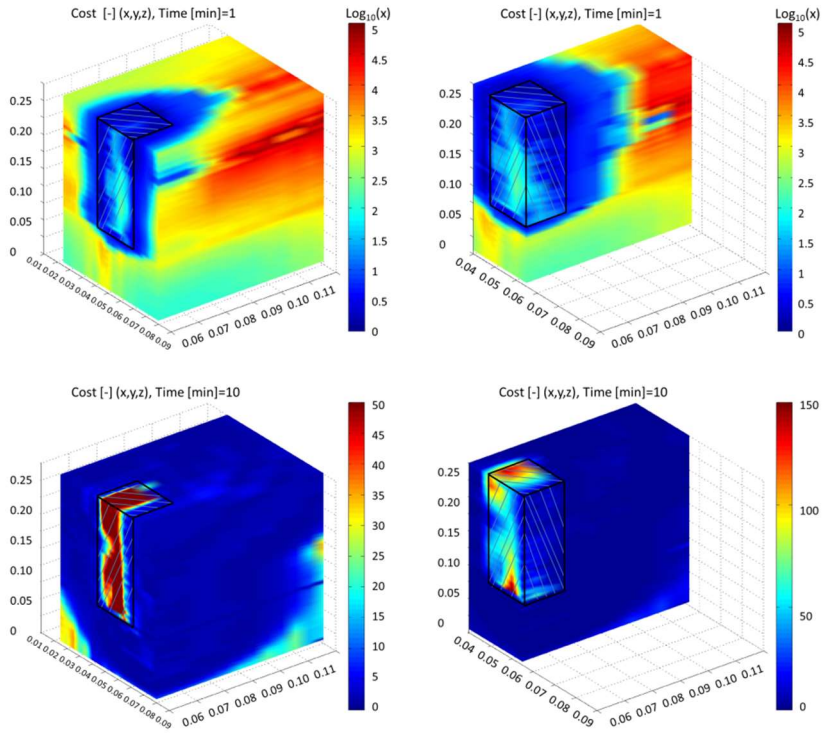

Fig. 8 Local unit exergy cost at minutes 1 and 10.

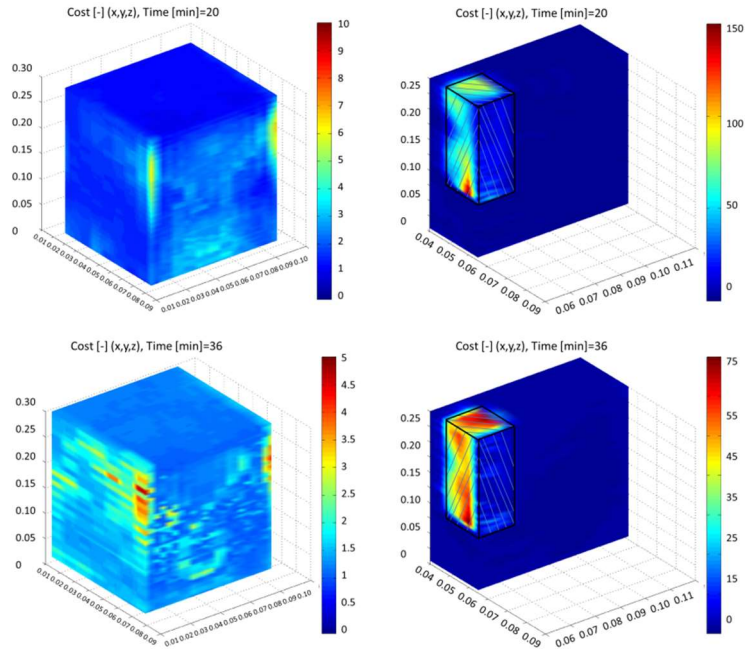

Fig. 9 Local unit exergy cost at minutes 20 and 36.

Fig. 9 shows that at the end of the heating process, high temperatures allow a good conversion of microwaves into heat with a rather low irreversibility, thereby producing an important decrease in the local unit exergy cost. Besides, the highest local unit exergy costs remain concentrated in the susceptor and relative high values also appeared in the glass corners. It should be noted that, as said before, local unit exergy cost quantifies the efficiency (actually, the inefficiency) of the history of the process. Heating at the beginning was inefficient, what leaded to very high values of unit exergy cost. When temperature increases and local efficiency also does, aggregated 'historical' efficiency increases, what leads to a

reduction of unit exergy cost. Highest values of cost appear in the areas located away from the susceptor and in the susceptor itself. This fact suggests one to make changes in the system affecting the susceptor: although many possibilities appear, the one that will be tested in next section will be to change the susceptor position.

To finish this section it is interesting to analyze a question related to the implementation of the methodology; in particular, how time step affect results. After a sensitivity analysis, time step for calculations was fixed equal to 0.037 minutes. Table 4 shows the value of unit exergy costs in the two selected points (see Fig. 3) at minutes 1 and 36 of the simulation for the base time step (0.037 minutes) and for a time step bigger and smaller. It can be seen that increasing time step affect significantly the values, where decreasing it has a negligible effect.

Time step	Local unit cost k^* [W/W] Point 1		Local unit cost k^* [W/W] Point 2	
	Initial	Final	Initial	Final
Base	2548.13	1.42	902.08	1.45
Base +15%	2735.65	1.67	968.46	1.71
Base –15%	2543.85	1.41	901.43	1.45

Table 4. Effect of time step on local unit exergy cost.

4. Effect of SiC susceptor position

When susceptor location is modified, the electromagnetic field inside the microwave cavity varies and different heating patterns are produced. This leads to important variations in the local exergy efficiencies, local unit exergy consumptions and local unit exergy costs. In this section, four different susceptor positions are compared (base case and B to D). The 3-D simulations are presented at 5 minutes, when glass was fully activated by microwave heating. Besides, the time evolution of the two representative points 1 and 2 (see Fig. 3) is also shown.

4.1 Local exergy efficiency

Fig. 10 shows the values of local exergy efficiency for the four cases. In case A, the efficiency found is above 60% only in zones nearby the susceptor. In case C, more zones reached those efficiencies. However, these cases are quite far from those efficiencies obtained in case B or case D with the highest values. In [43], locations B and D were proposed as the most suitable cases to perform the cullet glass heating process according to the temperature profiles found. Now, the local exergy cost analysis confirms this conclusion and clearly demonstrates that case B is the location which produces the highest efficiency.

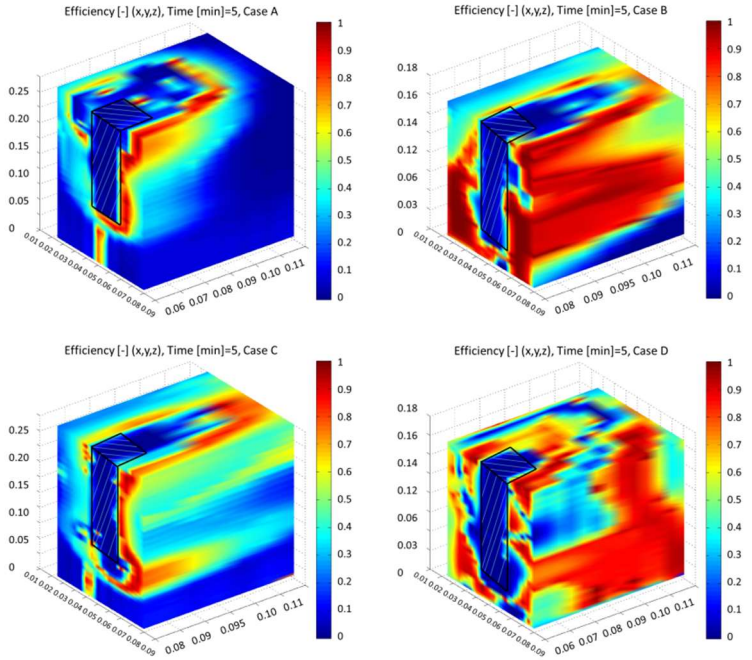

Fig. 10 Local exergy efficiency in all susceptor positions at minute 5.

Exergy efficiency evolution for these selected points in the microwave cavity was analyzed for cases A to D. Fig. 11 shows the results along time during the simulation, as well as point coordinates (also represented in Fig. 3). In case A, the exergy efficiency increased from minute 5 until minute 15 in both points. Then, it remained almost constant; however, by the end of the simulation, efficiency decreased, especially in point 2. The pattern for case C is almost the same. On the other hand, in cases B and D the efficiency constantly increased in the cullet along the heating process, especially for point 1. Nevertheless, as shown in Fig. 10, case B contains more volume elements with efficiency above 80%. Despite the aforementioned differences, it can be seen how all points and cases showed a quite similar pattern: at the beginning, efficiency was low due to low temperatures; afterwards it increased and kept in a high value during a time; finally, efficiency could decrease because exergy was being provided but the useful effect (increment of exergy due to increment of temperature) decreased.

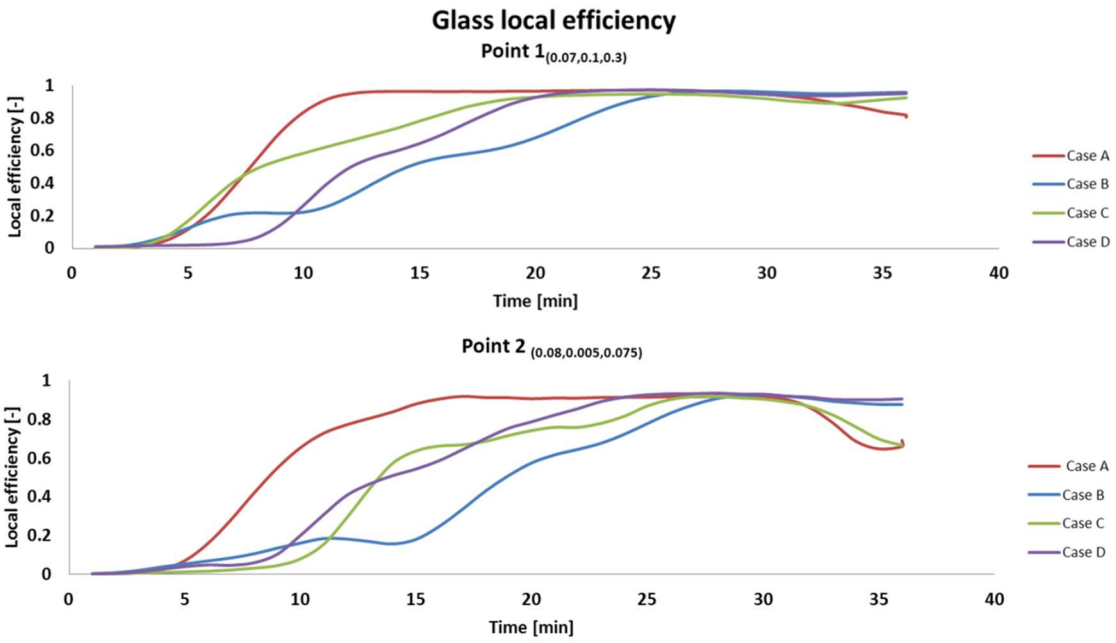

Fig. 11 Local exergy efficiencies of selected points (location inside of the applicator, dimensions in m).

4.2 Local unit exergy consumption

In Fig. 12, the total local unit exergy consumption in cases A-D was compared at five minutes of simulation, which is approximately the period with higher exergy activity between the susceptor and cullet glass. In cases A, C and D the local exergy consumption in susceptor and surroundings is higher compared with case B, what confirms that this case is the best one. Furthermore, this case shows a uniform distribution of the unit exergy consumption, which is an indicator of a more efficient process.

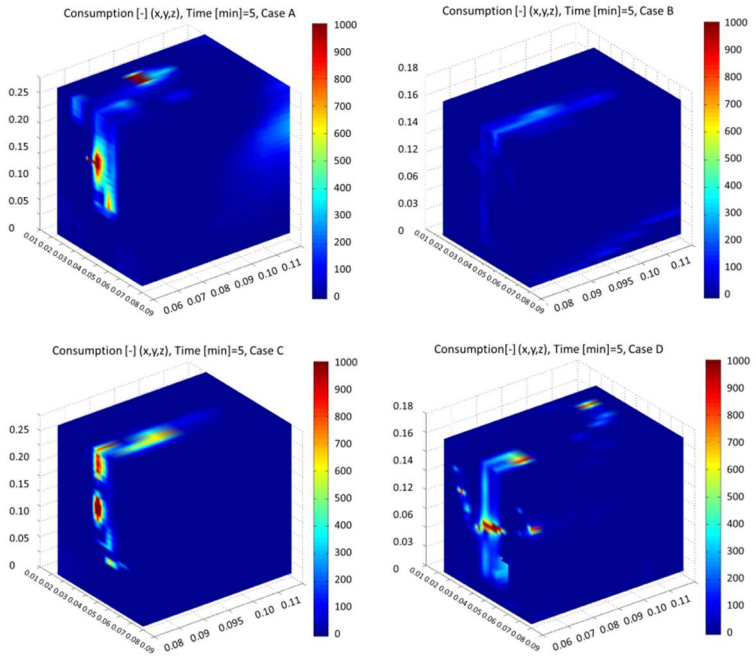

Fig. 12 Total local unit exergy consumption in all susceptor positions at minute 5.

Time evolution of local unit exergy consumption at the same points 1 and 2 is presented next. Fig. 13 shows first the local unit exergy consumption by microwaves (κ_{MW}). In the graphs on the right, the scale of y axis has been reduced to see better the values at the end of the process. This figure shows that at the beginning of simulation, in point 1, cases A and C consumed a quite high amount of exergy from microwaves (400 units and 600 units respectively). On the contrary, cases B and D initiated at values around 150 units. In point 2, however, the only case with high unit exergy consumption of microwaves is D. These marked differences in the initial consumption are provoked by the susceptor locations and their corresponding glass activation times. Those high values are due to the irreversibility of applying good quality energy (microwaves) for heating at temperatures rather close to the environment. However, at the end of the process and elevated temperatures all cases (except case A) have values of unit exergy consumption of microwaves lower than 1; this is possible because microwaves are not the only exergy source to produce the unit exergy consumption.

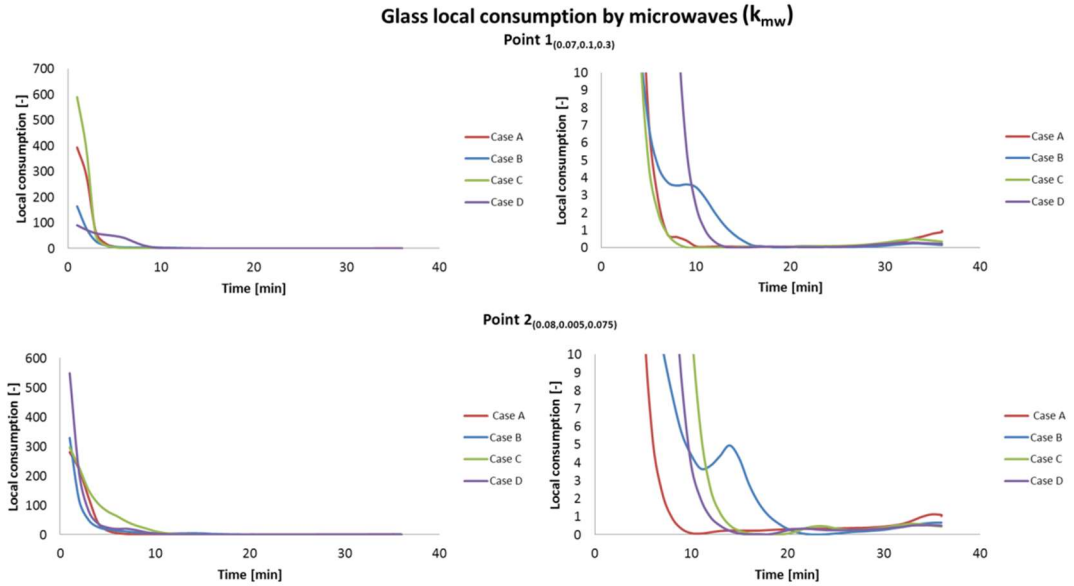

Fig. 13 Local unit exergy consumption of microwaves, κ_{MW}, of selected points (location inside of the applicator, dimensions in m).

The evolution of unit exergy consumption by heat conduction (κ_q) for all the cases can be seen in Fig. 14. When compared to the previous Figure, it clearly shows that during the first minutes the unit exergy consumption of heat conduction can be neglected compared to the unit exergy consumption of microwaves. However, at the end of the simulation the contribution of heat conduction equals or slightly overcomes the magnitude of the contribution of microwaves.

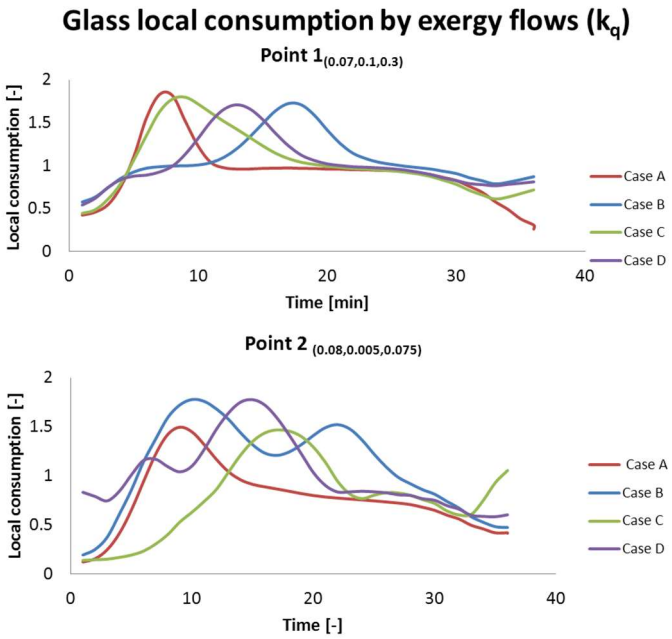

Fig. 14. Local unit exergy consumption of heat conduction, κ_Q, of selected points (location inside of the applicator, dimensions in m).

To sum up, local unit exergy consumption provides similar information as local exergy efficiency (it is the inverse rate) but it is also able to separate the origin of the source of that consumption (microwaves or heat conduction).

It should be stressed that both exergy efficiency and unit exergy consumption measure the use of the resources in specific time and space for the cullet melting simulation but they do not consider the accumulated irreversibilities produced during the whole melting. This means that if one wants to take into account the history of the process, the local unit exergy cost analysis has to be applied.

4.3 Local unit exergy cost

Local unit exergy cost for all cases at minute 5 is shown in Fig. 15. It can be seen that cases B and D concentrate higher values (about 150) of local unit exergy costs on the top of SiC susceptor, being in case B displaced to the nearby cullet (this means heating is delayed with respect the alternative positions of the susceptor). For cases A and C, local unit exergy cost is more evenly distributed along the susceptor surface. In case A, areas with high value of unit exergy cost also appear in the area located at high distance from the susceptor. This effect also appear, in case C, although values reached are much lower.

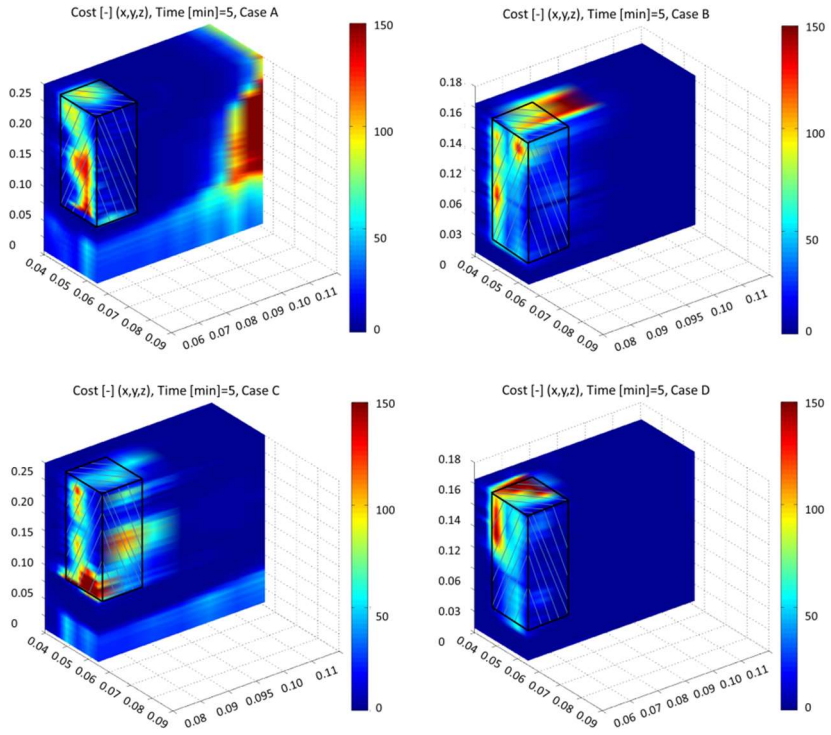

Fig. 15 Local unit exergy cost in all SiC positions at minute 5.

Figure 16 shows the time evolution of unit exergy cost in the benchmarked points. Again, zoom has been applied in figures on the right to show the cost evolution after the starting period. In cases C and D a higher local unit exergy cost at the beginning of the simulation was found with respect to cases A and B. However, in the period of 5 to 10 minutes in all cases the local unit exergy cost decreased sharply from the magnitude order of 10^3 to 10. At the process end for all the cases the local unit exergy cost was in the range from 1.3 to 1.4. Anyway, a rather similar path with the unit exergy consumption by microwaves is found (Figure 13), according to the F-P approach taken for the cost analysis. One thing is also true: local exergy cost values at the same point and time are usually higher than their respective unit exergy consumption rates, because they take into account the history of the heating process whose efficiency usually increases along time.

Finally, Table shows the initial and final values of the local unit exergy cost for each case in the checked points. At the end of the simulation, case B obtained the lowest local unit exergy cost, followed by case D. Although the two analyzed points are only an example and they do not represent the overall behavior of the cullet, this result confirm and reinforce the conclusions found with exergy efficiency in previous sections as well as results obtained with exergy transfer in [43].

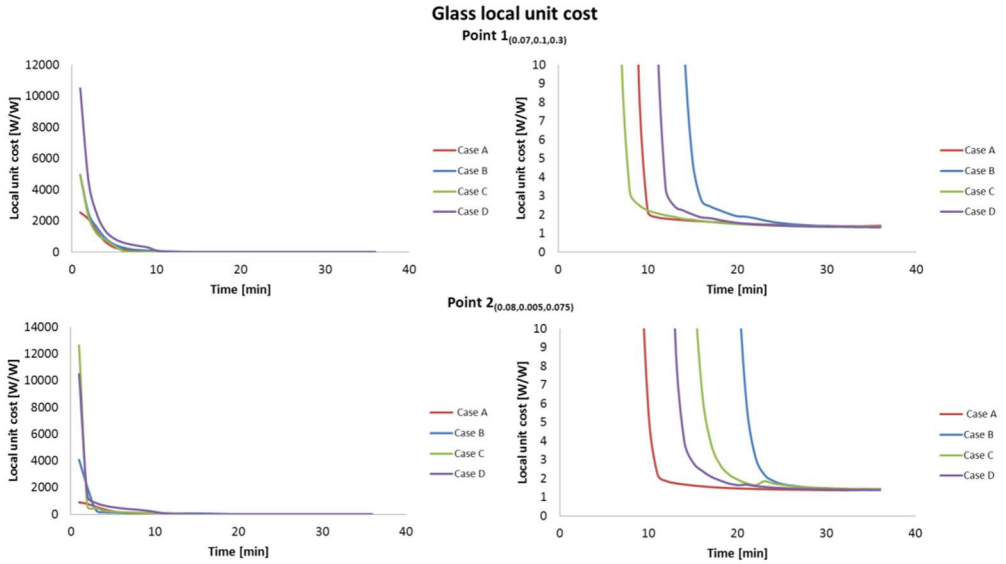

Fig. 16 Local unit exergy cost of selected points (location inside of the applicator, dimensions in m).

Case	Local unit cost k^* [W/W] Point 1		Local unit cost k^* [W/W] Point 2	
	Initial	Final	Initial	Final
A	2548.13	1.42	902.08	1.45
B	4967.3	1.33	4086.2	1.38
C	4940.1	1.36	12639	1.44
D	10511	1.34	10496	1.39

Table 5. Local unit exergy cost.

5. Conclusions

In this work, a local exergy analysis of a cullet glass melting process by using a susceptor (with different positions) has been performed. The approach includes the computation of local exergy efficiency and unit exergy consumptions (both by microwave and by conduction heat transfer) at any position and time of the system, as well as the 'path' of cost formation during the glass heating process. Results confirm the main conclusions previously obtained by modeling and exergy transfer analysis, but the use of the concepts of efficiency and cost allows one to go beyond by seeing new and clearer details.

In particular, the analysis shows that unit exergy consumption due to exergy flows (heat transfer) is negligible during the first 20 minutes compared to the unit exergy consumption due to exergy supplied by microwaves. Besides, the susceptor located as in cases A, C and D locally produces higher unit exergy consumptions and in consequence higher unit exergy cost than case B. In the analyzed selected points, reductions in the final local unit exergy cost of 1% to 6% were found when susceptor is located as in case B. In batch processes, even such low percentage of savings is important because along the time it accumulates significant energy consumptions that can be avoided. It is also noteworthy that locating the susceptor as in case B not only reduces the use of energy sources but also increase the quality of the product due to lower generation of the technically known as hot spots.

Besides, results show that efficiency is lower at the beginning of the heating process, due to higher irreversibility that appears when high quality energy (microwaves) is used for

heating slightly above ambient temperature, since glass is not activated yet, but then a fast reduction up to very good efficiencies is found in the process at moderate times, which is representative of this rapid heating method in the industry. This issue suggests that, if possible, other heat sources may be used in that first stage (e.g. preheating with waste heat). It should be emphasized that this result can be only observed by using exergy efficiency, because energy analysis is not able to quantify this different energy quality.

Along with the results related to the specific case, a main conclusion of the paper is that it is proved that the methodology can be applied to a realistic 3-D example of microwave heating for melting glass on just half an hour, and not only to a rather simplified case [41], and may be a tool for guiding in the search of more efficient designs. The basic motto of this search is to detect where and when low efficiency and/or high unit exergy costs appear, and then to try to modify the design in order to avoid or minimize these drawbacks.

Finally, it should be highlighted that, once the electromagnetic/thermal model has been solved, additional effort required for calculating exergy transfer, local exergy efficiency and local unit exergy cost is relatively low. Accordingly, it would be interesting to continue the application of this sequential approach (applying local exergy efficiency, unit consumptions and costs) to any other kind of energy systems.

Nomenclature

a	Specific non-flow exergy	J/kg
a^*	Specific non-flow exergy cost	J/kg
A	Non-flow exergy	J
A^*	Non-flow exergy cost	J
$\dot{b}$	Volumetric exergy flow	W/m^3
$\dot{B}$	Flow exergy	W
$\dot{B}^*$	Flow exergy cost	W
c	Specific heat	J/(kg·K)
$\dot{F}$	Fuel	W
$\dot{I}$	Irreversibility	W
k	Thermal conductivity	W/(m·K)
k^*	Unit exergy cost	W/W
$\dot{P}$	Product	W
T	Temperature	C
t	Time	s
x	Coordinate reference	m
y	Coordinate reference	m
z	Coordinate reference	m
Greek Symbols		
ρ	Density	kg/m^3
κ	Unit exergy consumption	-
η	Exergy efficiency	-
Subscripts and superscripts		
0	Reference or free-space properties	
a	Non-flow exergy	

b Exergy
e External
D Destroyed
i Space step
j Space step
k Space step
MW Microwave
n Time step
Q Heat transfer exergy flow

Acnowledgments

The first author acknowledges the support from Mexican "Consejo Nacional de Ciencia y Tecnologia" (CONACYT) through the scholarship number 25712. This work has been carried out with the support of grant of the "Secretaría de Educación Pública" (SEP) and the Mexican Government.

References

[1] Szargut J. Exergy Method: Technical and Ecological Applications (Developments in heat transfer).WitPress: 2005.

[2] Kotas J. The exergy method of thermal plant analysis. Butterworths: 1985.

[3] Dincer I, Cengel Y. Energy, entropy and exergy concepts and their roles in thermal engineering. Entropy 2001;3:116-49.

[4] Tribus M., Evans RB. A contribution to the theory of thermoeconomics. Technical report, Report No. 62-63; Department of Engineering, UCLA: Los Angeles, CA, USA, 1962.

[5] Lozano M., Valero A. A general theory of exergy saving: On the exergetic cost. AES ASME Book H0341C.

[6] Lozano M., Valero A. Theory of the exergetic cost. Energy 1993;18(9): 936-960.

[7] Torres C. Symbolic thermoeconomic analysis of energy systems. Exergy, energy system analysis and optimization 2009; 2(1):61-82.

[8] Tsatsaronis G. Thermoeconomic analysis and optimization of energy systems. Progress in Energy Combustion Science 1993;19:227-57.

[9] Rosen M., Bulucea C. Assessing electrical systems via exergy: a dualist view incorporating technical and environmental dimensions. In: Proceedings of the 6th WSEAS International Conference on Engineering Education, vol. 1., 2009. pp.116-23.

[10] Rosen M., Bulucea C. Using exergy to understand and improve the efficiency of electrical power technologies. Entropy 2009;11: 820-35.

[11] Petela R., Piotrowicz A. Exergy of plasma. Arch termodyn. spalania 1977;8:381-91.

[12] Ranjbaran M., Zare D. Simulation of energetic and exergetic performance of microwave-assisted fluidized bed drying of soybeans. Energy 2013;74:484-93.

[13] Strušnik D., Avsec J. Artificial neural networking model of energy and exergy district heating mony flows. Energy and Buildings 2015;86:366-75.

[14] Strušnik D., Avsec J. Artificial neural networking and fuzzy logic exergy controlling model of combined heat and power system in thermal power plant. Energy 2015;80:318-30.

[15] Sharifzadeh M., Ghazikhani M., Niazmand H. Temporal exergy analysis of adsorption cooling system by developing non-flow exergy function. Applied Thermal Engineering 2018;139:409-18.

[16] Choi W., Ooka R., Shukuya M. Exergy analysis for unsteady-state heat conduction. International Journal of Heat and Mass Transfer 20018;116;1124–42

[17] Qing-lin C., Yao X. The thermodynamic background of exergy transfer. Power and Energy Engineering Conference (APPEEC), 2010;1:1-4.

[18] Soma J. Exergy transfer: A new field of energy endeavor. Energy Engineering 1985; 82:11-22.

[19] Chun-Zhen Q., Xin-Yao X., Zhao-Yun W. Description of exergy transfer in the two dimensional thermal conduction process. Journal of Engineering Thermophysics 2003;24:202-4.

[20] Lior N., Sarmiento-Darkin W., Al-Sharqawi HS. The exergy fields in transport processes: Their calculation and use. Energy 2006;31:553-78.

[21] Wu S-Y., Chen Y., Li Y-R., Zeng D-L. Exergy transfer characteristics of forced convective heat transfer through a duct with constant wall heat flux. Energy 2007;32;686–96.

[22] Wu S-Y., Li Y-R., Chen Y., Xiao L. Exergy transfer characteristics of forced convective heat transfer through a duct with constant wall temperature. Energy 2007;32;2385–95.

[23] Cheng Q., Zheng A., Song S., Wu H., Lv L., Liu Y. Studies on the Exergy Transfer Law for the Irreversible Process in the Waxy Crude Oil Pipeline Transportation. Entropy 2018;20;309; doi:10.3390/e20050309

[24] Wang J., Liu Z., Yuan F., Liu W., Chen G. Convective heat transfer optimization in a circular tube based on local exergy destruction minimization. International Journal of Heat and Mass Transfer 2015;90;49–57.

[25] Liu W., Liu P., Wang J.B., Zheng N.B., Liu Z.C. Exergy destruction minimization: A principle to convective heat transfer enhancement. International Journal of Heat and Mass Transfer 2018;122;11–21.

[26] Kurtbas I., Celik N., Dinçer I. Exergy transfer in a porous rectangular channel. Energy 2010;35;451–60.

[27] Hara S., Maxson AJ., Kawaguchi Y. Exergy transfer characteristics analysis of turbulent heat transfer enhancement in surfactant solution. International Journal of Heat and Mass Transfer 2019;130;545–54.

[28] Wu S-Y., Yuan X-F., Li Y-R, Xiao L. Exergy transfer effectiveness on heat exchanger for finite pressure drop. Energy 2007;32;2110–20.

[29] Wang L., Li N. Exergy transfer and parametric study of counter flow wet cooling towers. Applied Thermal Engineering 2011;31;954-60.

[30] Feng J-S., Dong H., Gao J-Y, Liu J-Y, Liang K. Exergy transfer characteristics of gas-solid heat transfer through sinter bed layer in vertical tank. Energy 2016;111;154-64.

[31] Zheng Y., Cai J-J., Dong H., Feng J-S, Liu J-Y. Experimental investigation of volumetric exergy transfer coefficient in vertical moving bed for sinter waste heat recovery. Energy 2019;167;428-39.

[32] Rangel VH., Usón S., Cortés C., Valero A. Local Exergy Cost Theory. In: ASME International Mechanical Engineering Congress and Exposition; 2004.

[33] Wang S., Chen Q., Yin Q., Hua B. Theoretical research on the transfer equation of exergy cost. Proceedings of ECOS 2002:207-14.

[34] Wang S., Chen Q., Yin Q., Hua B. Transfer equation of exergy cost and its application. Chinese science bulletin 2003;48(7):619-22.

[35] Pizzolato A., Sciacovelli A., Verda V. Transient local entropy generation analysis for the design improvement of a thermocline thermal energy storage. Applied Thermal Engineering 2016;101;622–29.

[36] Pina EA., Lozano MA., Serra LM. Thermoeconomic cost allocation in simple trigeneration systems including thermal energy storage. Energy 2018;153;170-84.

[37] Santos T., Valente MA., Monteiro J., Sousa J., Costa LC. Electromagnetic and thermal history during microwave heating. Applied Thermal Engineering 2011;31:3255-61.

[38] Misra RR., Sharma AK. On melting characteristics of bulk Al-7039 alloy during in-situ microwave casting. Applied Thermal Engineering 2017;111:660-75.

[39] Hong Y., Lin B., Li H., Dai H., Zhu C., Yao H. Three-dimensional simulation of microwave heating coal sample with varying parameters. Applied Thermal Engineering 2016; 93:1145-54.

[40] Acevedo L., Usón S., Uche J. Exergy transfer analysis of microwave heating systems. Energy 2014;68:349-63.

[41] Acevedo L., Usón S., Uche J. Local Exergy cost analysis of microwave heating systems. Energy 2015;80:437-51.

[42] Acevedo L., Usón S., Uche J. Numerical study of cullet glass subjected to microwave heating and SiC susceptor effects. Part I: Combined electric and thermal model. Energy Conversion and Management 2015;97:439-57.

[43] Acevedo L., Usón S., Uche J. Numerical study of cullet glass subjected to microwave heating and SiC susceptor effects. Part II: Exergy transfer analysis. Energy Conversion and Management 2015;97:458-69.

[44] Sutton W. Microwave Processing of Ceramic Materials. Am. Ceram. Soc. Bull. 1989;68:376-86.

[45] Chaliha R., Tiwari V., Gupta P., Annapurna K., Tarafder A., Karmakar B. Structure and dielectric properties of potassium niobate nano glass–ceramics. Journal of Materials Science: Materials in Electronics 2011;22(7):728-34.